Environ. Sci. Technol. **2001**, *35,* 2100−2107

Emission Factors of Carbon Monoxide and Size-Resolved Aerosols from Biofuel Combustion

CHANDRA VENKATARAMAN* AND G. UMA MAHESWARA RAO

Centre for Environmental Science and Engineering, Indian Institute of Technology, Bombay, Powai, Mumbai-400 076, India

This study reports emission factors of carbon monoxide and size-resolved aerosols from combustion of wood, dung cake, and biofuel briquette in traditional and improved stoves in India. Wood was the cleanest burning fuel, with higher emissions of CO from dung cake and particulate matter from both dung cake and briquette fuels. Combustion of dung cake, especially in an improved metal stove, resulted in extremely high pollutant emissions. Instead, biogas from anaerobic dung digestion should be promoted as a cooking fuel for public health protection. Pollutant emissions increased with increasing stove thermal efficiency, implying that thermal efficiency enhancement in the improved stoves was mainly from design features leading to increased heat transfer but not combustion efficiency. Compared to the traditional stove, the improved stoves resulted in the lower pollutant emissions on a kW h^{-1} basis from wood combustion but in similar emissions from briquette and dung cake. Stove designs are needed with good emissions performance across multiple fuels. Unimodal aerosol size distributions were measured from biofuel combustion with mass median aerodynamic diameters of 0.5−0.8 μm, about a factor of 10 larger than those from fossil fuel combustion (e.g. diesel), with potential implications for lung deposition and health risk.

Introduction

Biofuels (including wood, dried animal-dung cake, and crop waste) are used for cooking energy by about 110 million rural and 15 million urban households in India (*1*, *2*). The 1990 national consumption of biofuels was estimated at about 450×10^6 t yr^{-1} with a 59:18:23% division among fuelwood, dung cake, and crop waste, respectively (*2*). Rural income stratification, occupation structure, and the unreliability of the rural supply of petroleum fuels and electricity in India make an imminent transition away from biofuels unlikely (*3*). Biofuels are typically burnt indoors in small, open-chamber stoves without flues (*4*). This results in high exposures to aerosols (including respirable particles), associated toxic pollutants, and carbon monoxide (*5*−*10*). The high pollutant exposures have been associated with acute respiratory infection in children, adverse pregnancy outcomes in women, and chronic lung disease (*6, 7*).

Measurement of pollutant emissions from biofuel combustion, under standard laboratory conditions, has been made using two approaches, i.e., the "chamber" method (*11*, *12*) and the "hood" method (*13*−*16*). Both methods have employed a standard burn-cycle test (*17*) during which the amounts of fuel burnt and pollutants emitted are measured to estimate an emission factor in terms of mass pollutant emitted per mass fuel burnt. The chamber method involves measuring pollutant concentrations in a chamber during the burn-cycle test and estimating emission factors from a mass balance, which, in simplest form, assumes constant rates of fuel burn, emission and ventilation, and complete mixing. Size-dependent particle loss rates to the chamber walls and deviation from the assumptions of constant burn and emission rate result in uncertainties in the estimated particle emission factors. The hood method involves entraining the emissions in a duct through a hood, drawing an isokinetic sample using a probe, and directly collecting the pollutant or measuring its concentration. Here, particulate species emissions could be underestimated by high-temperature filtration or may be overestimated by addition of the fraction collected by cold-trapping, e.g., Modified EPA Method 5 (*18*). This would not accurately reflect the gas−particle partitioning that occurs at temperatures and dilutions present in typical indoor environments. Also, filtration and trapping do not allow size resolution of the aerosol emissions, which are needed to refine lung dose and health risk calculations.

Incomplete combustion of emitted organic compounds is expected to contribute significantly to aerosol formation during biofuel combustion, because of the high fuel volatile matter content and the low combustion temperatures. Emission factors of particulate organic matter were shown to increase with decreasing combustion temperature and with increasing volatile matter content in coal (*19*). The accurate measurement of aerosol size distribution requires sufficient dilution, cooling, and residence time for quenching aerosol dynamics and chemistry in the postcombustion gases before particle collection (*20*, *21*).

In view of the adverse health effects of biofuel combustion emissions on the large user population and the need for developing cleaner burning systems, the objectives of this study included the following:

(i) to design and build a dilution sampler suitable for accurate aerosol size-distribution measurement from biofuel combustion,

(ii) to measure emission factors of CO and, for the first time, size-resolved aerosols from stove−fuel systems commonly used in India, and

(iii) to relate CO and aerosol emission factors to combustion and fuel parameters.

Experimental Methods

Dilution Sampler. A dilution sampler was designed to meet the considerations needed for accurate aerosol size-distribution measurements based on those identified for organic aerosols (*20*). These include sufficient dilution, cooling, and residence time to achieve the quenching typical of indoor environments and use of stainless steel (SS-304) with Teflon gaskets to avoid organic species contamination (*22*). Since biofuel combustion is natural-convection driven, it was important that emissions entrainment into the hood, by the fan, should not exert a draught that could alter combustion conditions and consequently the emissions. The sampler consists of a rectangular hood (0.8 m × 1.3 m), large enough to cover the largest stove and entrain the emissions without spillage. This is connected to a duct (i.d. = 0.163 m) with an induced draught fan at its end (Figure 1), exhausting the emissions to the outside. Air is drawn from the duct through

* Corresponding author phone: +91-22-576-7856; fax: +91-22-572-3480; e-mail: chandra@cc.iitb.ac.in.

10.1021/es001603d CCC: $20.00
Published on Web 04/11/2001

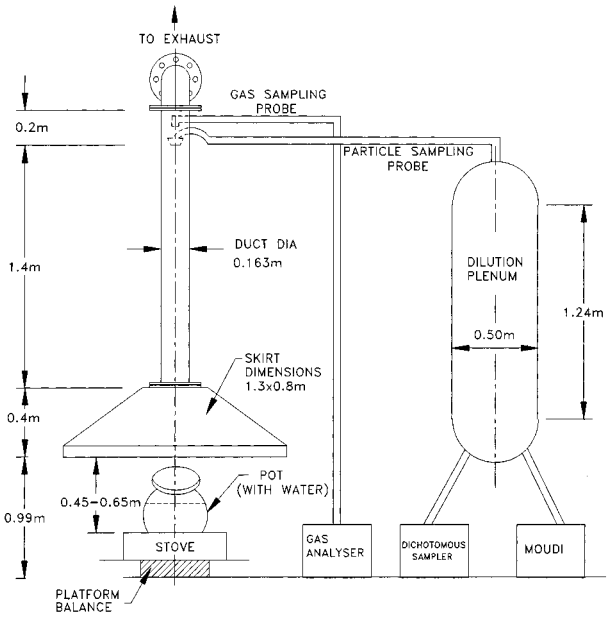

FIGURE 1. Schematic of the dilution sampler.

an isokinetic sampling probe, placed 8 diameters downstream of the duct inlet and 1.5 diameters upstream of a bend for fully developed flow. A dilution plenum provides additional residence time for complete quenching and has four ports for connection to particle samplers.

The entrainment of lab air into the duct along with the combustion emissions gave average dilution ratios of 40−60 (calculated from measured combustion and duct temperatures) and allowed cooling of the combustion gases to 2−3 °C above ambient in the dilution plenum. The extraction flow rate in the duct was adjusted by the fan rpm to provide this dilution, subject to a maximum of velocity of 1.5 ms^{-1} (*14*). The midpoint velocity was measured by a platinum hot-wire sensor, calibrated for total flow rate using a standard orifice calibrator. A duct diameter of 0.163 m was provided resulting in an average volume flow rate of 0.022 $m^3 s^{-1}$ and Reynolds number of 10 800 (at 50 °C). Plenum residence times, calculated for 99% condensation of semivolatile organic species, assuming heterogeneous condensation on an assumed particle number distribution, from a coal boiler (*30*) ranged 280−420 s at the dilution ratios of 40−60. The pollutant sampling rate (46.7 L min^{-1}), determined by the particle collection instruments, and an average dilution ratio of 50 (residence time of 350 s) allowed sizing of the plenum (0.272 m^3) and the nozzle diameter (25.7 mm) required for isokinetic sampling.

Dilution Sampler Testing. The extraction flow rate provided by the induced draught fan and the stove-hood distance were optimized so that natural draught conditions were maintained. The natural burn rate was determined in experiments on the roof of the laboratory (*22*). The burn rate was measured in experiments using extraction rates of 0.01−0.03 $m^3 s^{-1}$ and stove-hood distances of 0.35−0.65 m. Larger extraction rates and stove-hood distances less than 0.45 m resulted in burn rates enhanced above the natural burn rate. Stove-hood distances greater than 0.65 m resulted in emissions spillage out of the hood. Therefore an optimum extraction rate of 0.022 $m^3 s^{-1}$ and stove-hood distance of 0.45 m were chosen. The sampler was designed to minimize particle losses, and visual inspection did not show significant particle deposition or retention.

Fuels and Stoves. Fuels used in this study, included wood (*Acacia nilotica*, local names keekar or babul), dung cake, and biofuel briquettes. Wood and dung cake are widely used throughout India. While crop waste accounts about 23% of the biofuel use, the wide variety (rice stalk, mustard stalk, groundnut stalk, etc.) and regional variation warranted determining the predominant crop waste and stove combinations in use, before emissions measurement, in a future study. Biofuel briquette was chosen to assess the effect of densification on potential improvement of combustion and emission characteristics of widely used loose biomass (e.g., leaves, rice husk, pine needles). Wood of diameter 2−4 cm was split and cut into pieces approximately 20−25 cm in length. Dung cakes of diameter 15−20 cm were divided into quarters. Briquettes were made with crushed pine needles, dung, and starch binder using an extruder (*23*) and were cylindrical (H = 10 cm, o.d. = 6 cm) with an axial hole (i.d. = 1.5 cm). Fuel proximate and ultimate analysis (Table 1) showed that dung cake and briquette had higher ash content than wood. On a moisture- and ash-free basis, all the fuels had about the same volatile matter, fixed carbon, and oxygen content, implying that differing ash contents are likely to affect combustion. The net heating value for wood at 16 MJ kg^{-1} was higher than that of about 10 MJ kg^{-1} for the other fuels. Stoves used (Figure 2) included three one-pot stoves (metal S1, fired-clay S2, traditional mud S3) and one two-pot fired-clay stove, S4. Stoves S1, S2, and S4 were designed for improved thermal efficiency, while S3 was a traditional, U-shaped, mud stove. Stove design parameters likely to affect combustion (Table 2) include the combustion chamber or fire-box volume, air inlet areas (primary air from bottom of the fuel-bed through the grate and secondary air from above the fuel-bed through the fire-box opening), and grate-to-pot height.

The burn-cycle, adapted from the VITA water-boiling test (*17*), involved heating 1.5 kg of water from room temperature to its boiling point and simmering for 5 min. This includes emissions from both low- and high-power phases, likely to be encountered in real cooking practice, giving a realistic emission factor. The time for accomplishment of the burn-cycle corresponded to the particle sampling times (19−31 min), which had to be kept low to avoid overloading the particle sampling substrates. The stove−fuel−pot assembly (fitted with a thermometer) was placed on a platform balance to record weight (and hence fuel burn rate) every minute.

TABLE 1. Fuel Proximate and Ultimate Analysis, Moisture and Ash-Free, and Moisture and Mineral Matter-Free Basis

	wood		dung cake		biofuel briquette	
proximate anal.	%	maf[c] (%)	%	maf (%)	%	maf (%)
moisture (%)	5.30[a]		7.82		7.34	
ash (%)	3.14[b]		31.46		18.88	
volatile matter (%)	71.59	78.1	47.41	78.1	54.50	74.0
fixed carbon (%)	20.00	21.9	13.30	21.9	19.28	26.0
net heating value (MJ/kg)	16.21		9.79		10.30	

	wood		dung cake		biofuel briquette	
ultimate anal.	%	mmf[d] (%)	%	mmf (%)	%	mmf (%)
moisture (%)	5.30		7.82		7.34	
mineral matter (%)	3.41[b]		34.61		20.77	
carbon (%)	49.91	54.8	32.97	58.7	36.94	51.3
hydrogen (%)	4.65	4.9	4.50	8.41	4.01	5.6
nitrogen (%)	0.26	0.3	1.32	2.35	0.89	1.3
sulfur (%)	0.32	0.4	0.12	0.20	0.69	0.9
oxygen (%)	36.16	39.6	18.68	33.3	29.37	40.9

[a] Values are the mean of two values. [b] Ash corrected for moisture content from proximate analysis would compare with mineral matter from ultimate analysis. [c] Moisture- and ash-free basis. [d] Moisture- and mineral matter-free basis.

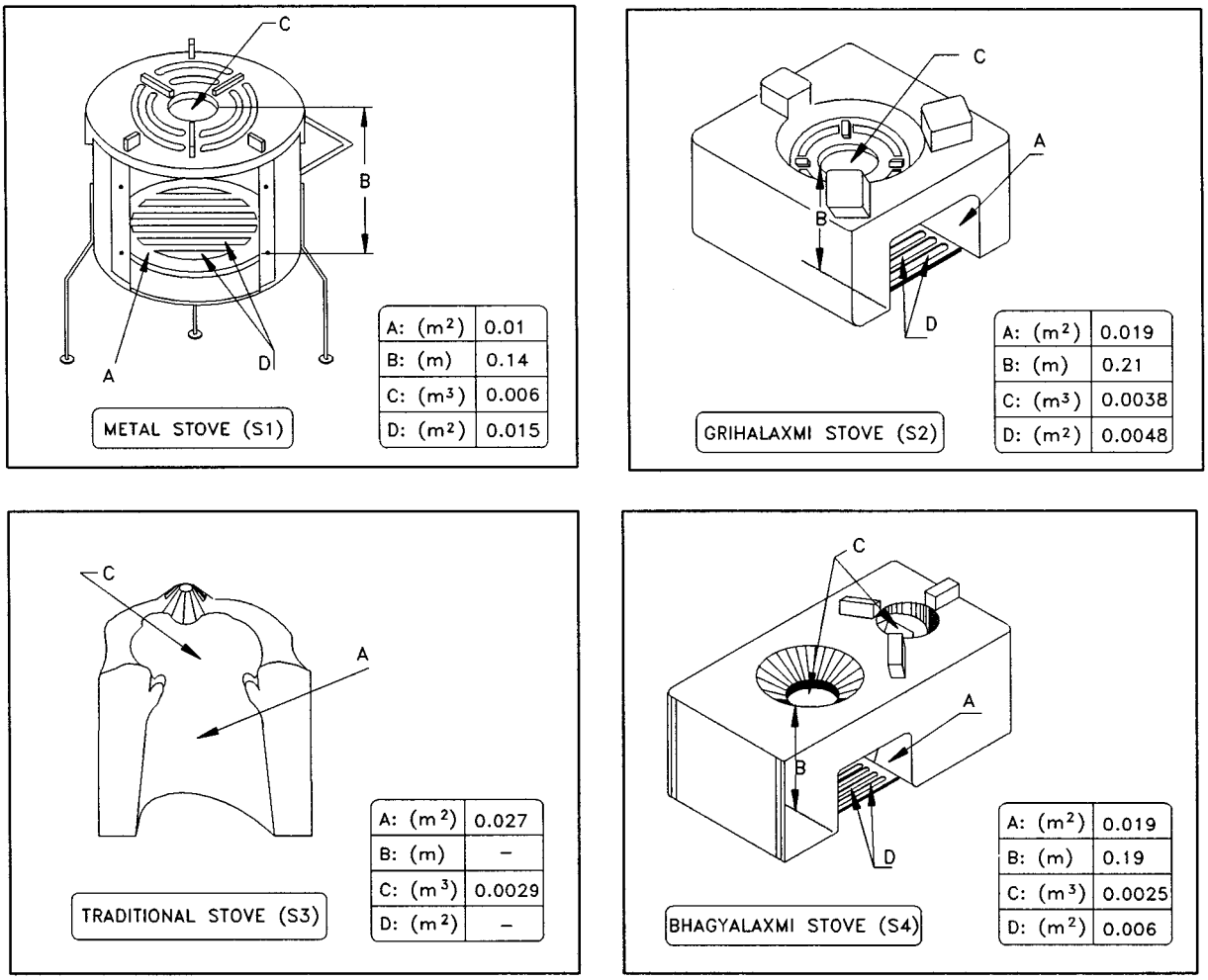

FIGURE 2. Schematic of the stoves (a) improved metal stove, S1; (b) improved one pot fired-clay stove, S2; (c) traditional mud stove, S3; (d) improved two pot fired-clay stove, S4, showing the fire box opening (A), grate to pot bottom distance (B), combustion chamber volume (C), and grate air inlet area (D). The thermocouple was placed 2−3 cm below the top of the flame.

TABLE 2. Stove Features and Design Parameters

name	description	combustion chamber vol (m^3)	grate to pot-bottom distance (m)	grate air-inlet area (primary air) (m^2)	fire box opening (secondary air) (m^2)	rated thermal efficiency[a] (%)	fuel used
S1, metal (improved)	portable, single pot, top-slotted plate, bottom grate	0.0060	0.14	0.0150	0.010	28−30	wood, dung cake
S2, fired clay (improved)	single pot, cast iron, top and bottom grate	0.0038	0.21	0.0048	0.019	28−30	wood, dung cake, biofuel briquette
S3, mud (traditional)	single pot, U-shaped, three pot raisers, no top or bottom grate	0.0029	0.24[b]	no grate	0.027	15−20	wood, dung cake, biofuel briquette
S4, fired clay (improved)	two pots, top and bottom grate	0.0025	0.19	0.0060	0.019	28−30	wood, dung cake

[a] As provided by the manufacturer. [b] Floor to pot-bottom distance.

Pollutant Sampling and Data Inversion. As the focus of this study was health-related source characterization, emission factors of CO and size-resolved aerosols were measured. A micro-orifice uniform deposit impactor (MOUDI model 110, MSP Corporation, USA), operating at a flow rate of 30 L min^{-1} was used to obtain a size fractionated particle sample. The MOUDI has 50% cut-point aerodynamic diameters of 10, 5.6, 3.2, 1.8, 1.0, 0.56, 0.32, 0.18, 0.097, and 0.056 μm on stages 1−10, respectively, and collects particles smaller than 0.056 μm on a 37-mm quartz fiber afterfilter. Flow rate and leak checks were conducted on the impactor before and after each experiment, and the 9th stage stagnation pressure was monitored using a pressure gauge. Aluminum foils of 47 mm diameter were coated with silicone by solvent evaporation of 20 μL of 4% silicone in cyclohexane solution, which was spread using a clean glass rod. All substrates were conditioned, before and after sample collection, for 8 h at about 25 °C and 50% RH (in an air-conditioned room), and weighed on a microbalance (model BP211D, Sartorius, Germany) accurate to 10 μg. CO concentrations in the duct were recorded each minute using an electrochemical sensor based instrument (model 1400, IMR, USA). The sensor was zeroed

against room air and calibrated with a span gas of 1000 ppm CO in nitrogen. In addition, temperatures in the combustion zone, duct, and plenum and the midpoint velocity in the duct were recorded each minute by a data logger and downloaded to a computer.

The average particle concentrations measured during the burn-cycle were converted to emitted mass (g), multiplying by the total volume of air exhausted through the duct (corrected to standard temperature and pressure of 298 K and 1 atm), and to the emission factor (g kg^{-1}) dividing by the fuel burnt. CO concentrations, recorded each minute, were converted as above and added over the burn-cycle time to obtain the CO emission factor.

A least-squares error minimization procedure was used to invert the size distribution data from the MOUDI and obtain the best estimate mass median aerodynamic diameter (MMAD) and the geometric standard deviation. Background particle concentrations, measured to account for particles in the dilution air from the room, were between 0.001 and 0.01 of the MOUDI stage mass collected in a typical experiment and were therefore neglected.

Results and Discussion

Thermal Parameters. Thermal efficiencies ranged as follows: 14−20% for the traditional mud stove (S3), 21−26% for the improved fired-clay stoves (S2 and S4), and 31−33% for the improved metal stove (S1) (Table 3). The thermal efficiency difference from using different fuels was statistically significant only for S3, the traditional mud stove ($F = 10.1$; $p < 0.005$), with wood giving the lowest thermal efficiency of 14% and briquettes and dung of 19−20%. In previous studies (*25*, *26*), in contrast, traditional stoves showed virtually invariant thermal efficiency among various fuels (wood, dung cake, and crop waste). The traditional stove in this study, S3, had the largest floor-to-pot-bottom distance of 0.24 m. This resulted in the flame from wood combustion not touching the pot bottom and the consequent low thermal efficiency, probably from lower conductive and/or convective heat transfer from the flame to the pot. Unlike wood, the flames from dung cake and briquette, which packed the combustion chamber, touched the pot bottom and resulted in higher thermal efficiency. However, flame quenching from contact with the pot would affect emissions, described in following sections.

The power at which a given stove operated was fairly invariant, even when using different fuels (Table 3). As the goal of this study was to measure emission factors under conditions of realistic stove operation, we did not attempt to operate stoves over a range of power. In previous work, stoves operated over a power range showed an increase in thermal efficiency with power (*25*, *26*) or optimum thermal efficiency corresponding to a given power (*27*).

Effect of Biofuel Type on CO and PM Emission Factors. Particulate matter (PM) emission factors from various stove−fuel systems showed a good correlation with those of CO ($R^2 = 0.71$). This finding is consistent with previous studies, which reported a significant correlation between emission factors of CO and respirable particles (smaller than 5 μm) (*12*) and a weaker correlation with total particles measured by filtration (*11*, *25*, *26*) or by optical density (*13*).

Emission factors of CO ranged 8−9, 11−12, and 14−29 g kg^{-1}, respectively, from combustion of briquette, wood, and dung cake (Table 3). Also shown in the table are emission factors in terms of unit of useful heat input to the pot, which are obtained by dividing the mass of pollutant emitted by the product of fire power (kW), burn time (h), and thermal efficiency (dimensionless fraction) (Table 3 and Appendix). While the first emission factor E(CO) (g kg^{-1}) is useful for generation of emission inventories, the second E_Q(CO) (g $(kW\ h)^{-1}$) is a better estimate of the emissions to which the

TABLE 3. Summary of Thermal Parameters and Emission Factors of Aerosols and Carbon Monoxide

fuel	stove	no. of repeat expts	time of burn (min)	fuel used[b] (kg)	burn rate[c] (kg h^{-1})	fire power[d] (kW)	thermal efficiency (%)	combustion temp (°C)	dilution ratio	emission factors particles			
										PM		CO	
										g kg^{-1}	g $(kW\ h)^{-1}$	g kg^{-1}	g $(kW\ h)^{-1}$
wood	S1	4	26 ± 6[a]	0.21 ± 0.03	0.39 ± 0.05	1.7 ± 0.2	33 ± 6	483 ± 33	57 ± 6	1.2 ± 0.8	1.2 ± 0.8	12 ± 1	12 ± 5
	S2	4	25 ± 5	0.37 ± 0.03	0.60 ± 0.20	2.6 ± 0.7	25 ± 2	565 ± 35	47 ± 7	1.1 ± 0.2	1.8 ± 0.7	12 ± 3	17 ± 6
	S3	4	30 ± 3	0.44 ± 0.07	0.40 ± 0.13	2.9 ± 0.6	14 ± 2	568 ± 17	46 ± 8	2.8 ± 0.5	3.8 ± 0.7	11 ± 3	24 ± 6
	S4	4	24 ± 4	0.41 ± 0.05	0.90 ± 0.20	4.0 ± 0.8	26 ± 3	499 ± 43	53 ± 3	0.9 ± 0.3	0.8 ± 0.2	12 ± 2	12 ± 1
biofuel briquette	S2	4	19 ± 2	0.33 ± 0.05	1.05 ± 0.13	3.3 ± 0.4	21 ± 4	522 ± 33	40 ± 3	3.2 ± 0.9	3.2 ± 0.9	9 ± 1	14 ± 2
	S3	4	20 ± 3	0.34 ± 0.04	1.03 ± 0.15	3.7 ± 0.4	19 ± 2	591 ± 32	42 ± 7	4.8 ± 1.4	3.8 ± 1.0	9 ± 2	16 ± 4
dung cake	S1	4	31 ± 5	0.23 ± 0.04	0.44 ± 0.12	1.6 ± 0.3	31 ± 2	515 ± 42	56 ± 13	4.9 ± 1.6	3.5 ± 0.9	29 ± 2	28 ± 6
	S2	4	21 ± 5	0.28 ± 0.05	0.85 ± 0.13	3.0 ± 0.4	22 ± 3	650 ± 31	42 ± 9	4.4 ± 0.6	3.5 ± 0.5	18 ± 4	25 ± 6
	S3	4	23 ± 4	0.27 ± 0.06	0.73 ± 0.21	2.8 ± 0.5	20 ± 1	631 ± 51	43 ± 6	4.6 ± 0.6	3.2 ± 0.4	18 ± 2	24 ± 7
	S4	4	25 ± 2	0.36 ± 0.04	0.96 ± 0.19	3.0 ± 0.2	23 ± 1	672 ± 47	60 ± 7	3.9 ± 0.9	3.5 ± 1.2	14 ± 2	21 ± 3

[a] Uncertainties are one standard deviation from the mean of four samples. [b] Fuel used is on a moist basis. [c] Burn rate was calculated on dry basis. [d] Fire power is power used in calculation of emission factors in terms of unit heat input from the mean of four samples.

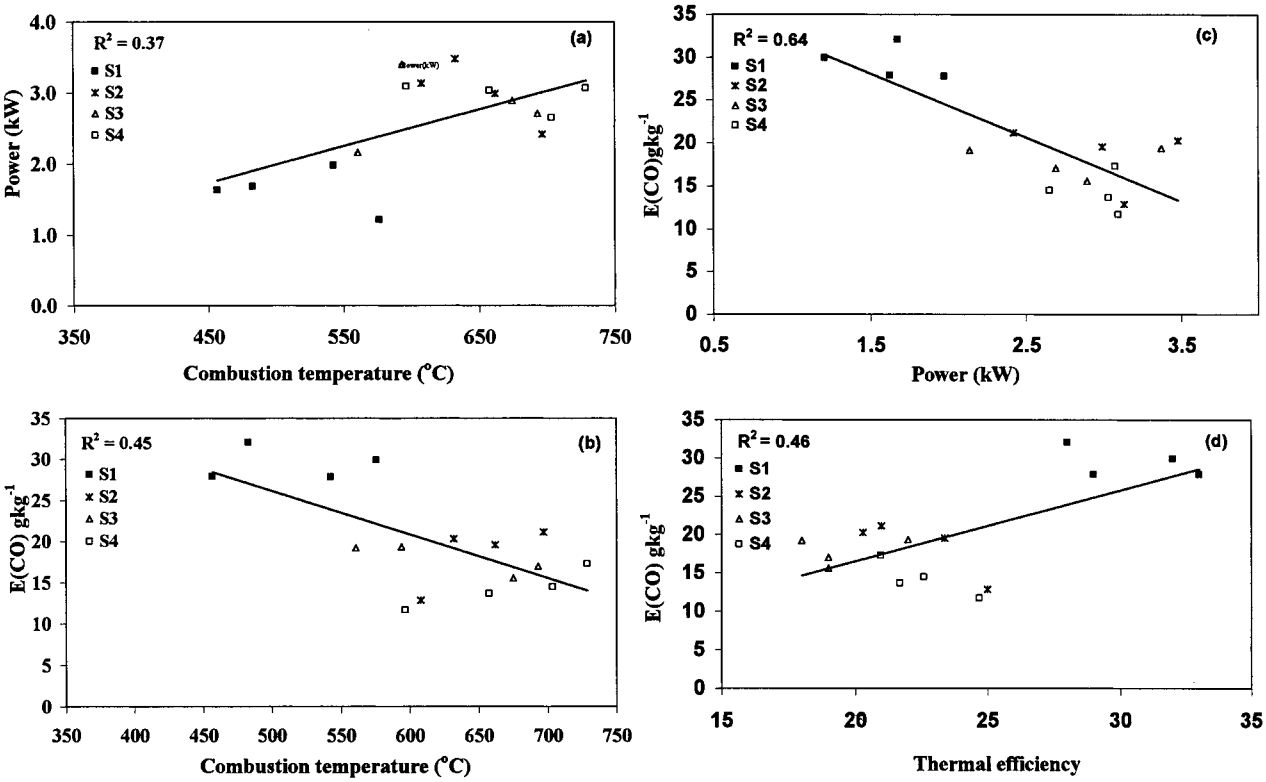

FIGURE 3. For dung cake combustion, the power increased with increasing combustion temperature (a). Emission factors of carbon monoxide increased with decreasing combustion temperature (b), decreasing power (c), and increasing thermal efficiency (d) of the stove−fuel system.

stove user would be exposed per unit useful heat input to the pot or accomplishment of a given cooking task. On the basis of this, dung cake was a more polluting fuel (E_Q(CO) = 21−28 g (kW h)$^{-1}$) than wood and briquette (E_Q(CO) = 14−15 g (kW h)$^{-1}$) and wood (E_Q(CO) = 12−24 g (kW h)$^{-1}$) with respect to CO, with high statistical significance (F = 53.5; p < 1.2E−11). This is consistent with previous studies in which the CO emission factor was seen to depend strongly on the fuel type (*16*).

Emission factors of particulate matter were obtained from the total mass measured on all stages of the MOUDI. They were 0.8−1.8, 2.1−2.2, and 2.4−3.7 g kg^{-1}, respectively, from wood, briquette, and dung cake combustion, in general agreement with those reported in earlier studies using filtration (*11*, *12*, *25*, *26*) or by optical density (*13*). The emission factors based on useful heat input were 0.8−3.8, 3.2−3.8, and 3.2−3.5 g (kW h)$^{-1}$, respectively, for wood, briquette, and dung cake combustion (Table 3). PM emissions factors were significantly higher from dung cake and briquette combustion (F = 10.8; p < 2E−4) than from wood combustion.

Biofuel briquette was used in this study to assess the effect of densification on potential improvement of combustion and emission characteristics of loose biomass. However, the briquettes in this study were made using pine needle dust (which contains resins) and cow dung binder, leading to fuel characteristics closer to dung cake than wood (Table 1) and, consequently, higher emissions. In future work, it would be of interest to study briquettes made of woody biomass with starch binder.

Effect of Stove/Combustion Parameters on CO and PM Emissions from a Given Biofuel. The variation in CO emission factor from combustion of a given fuel in the different stoves was statistically significant for dung cake (F = 25.2, p < 1.8E−05), whereas no such variation were obtained in case of wood (F = 0.3; p < 0.84) and briquette (F = 0.1, p < 0.8). There were trends in the emissions with stove power, combustion temperature, and thermal efficiency (Figure 3). Low-combustion temperatures occurred at low power (Figure 3a), especially for the metal stove S1 and traditional stove S3. The combustion temperature was measured using a K-type thermocouple, with the tip placed at the center of the combustion chamber in the flaming zone, about 2−3 cm below the top of the flame and corrected for radiation losses to the stove walls using measured wall temperatures (*28*).

Since dung cake had a low density and high ash content (31.5%, Table 1), the combustion chamber was filled first by the fuel and later by the residual ash, blocking the primary air inlet holes and limiting oxygen transfer. The restricted air supply resulted in the low-power, low-combustion temperature and the consequent high emissions. This smouldering combustion effect was most pronounced for the metal stove, S1 (lowest average combustion temperature of 514 °C and highest average CO emissions factor of 29 g kg^{-1}). In this stove, combustion was most dependent on the primary air as it had the smallest fire-box opening for secondary air (Table 2).

CO emission factors did not vary much for a given stove over its range of power, combustion temperature, and thermal efficiency. However, among stoves, the CO emission factor increased with decreasing combustion temperature (Figure 3b) and decreasing power (Figure 3c), indicating more incomplete combustion at lower powers of operation. CO emissions also increased with increasing thermal efficiency (Figure 3d), implying that stoves designed for improved thermal efficiency actually operated at decreased combustion efficiency accompanied by higher emissions. This trend, seen previously (*25*, *26*), has been attributed to the thermal efficiency being a product of the combustion and heat transfer efficiency. The increase in overall thermal efficiency in the improved stoves is mainly from design improvements leading

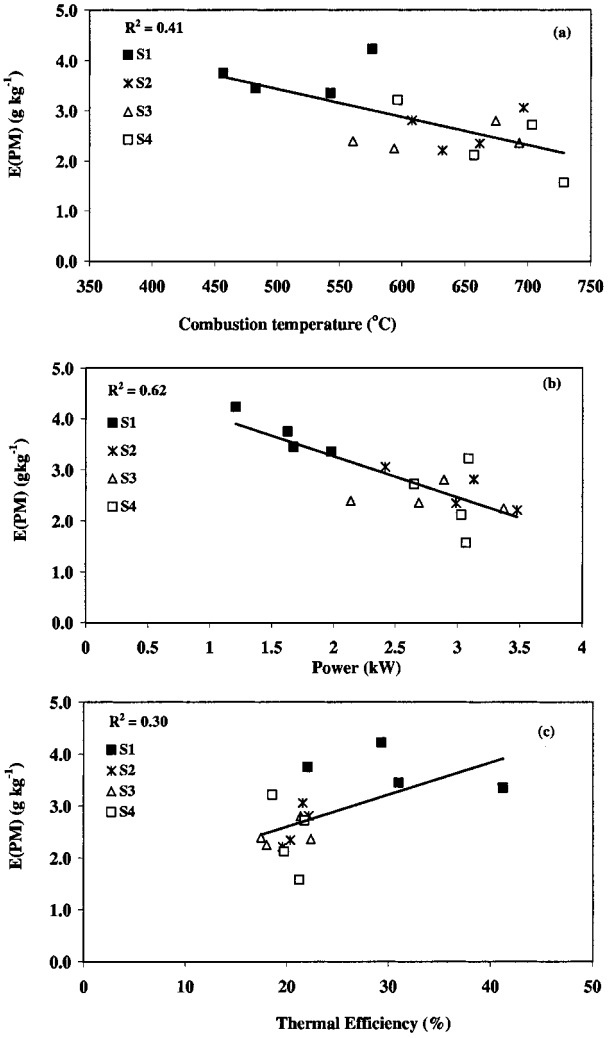

FIGURE 4. For dung cake combustion, emission factors of particulate matter increased with decreasing combustion temperature (a), decreasing power (b), and increasing thermal efficiency (c) of the stove−fuel system.

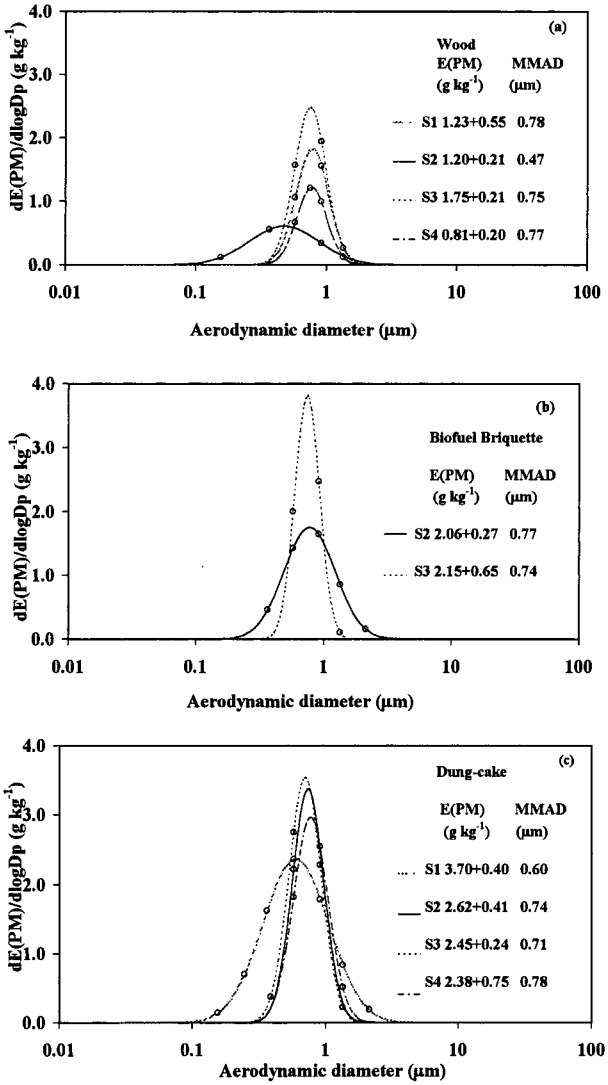

FIGURE 5. Particle mass size distributions from the combustion of wood (a), biofuel briquette (b), and dung cake (c) were all unimodal with mass median aerodynamic diameter in the range of 0.47−0.78 μm.

to an increase in heat transfer but not in combustion efficiency.

Comparing among stoves for a given fuel showed PM emissions from dung cake to be significantly higher from S1 than the other stoves ($F = 6.7$; $p < 7E{-}03$), from wood to be significantly lower from S4 than the other stoves ($F = 5.4$; $p < 0.01$), and from briquette to be independent of stove type comparing between S2 and S3. As with CO, the PM emissions factors for a given stove were similar over its range of operation and, among stoves, increased with decreasing combustion temperature (Figure 4a), indicating more incomplete combustion at lower temperatures. PM emission factors also increased with decreasing power (Figure 4b) and with increasing thermal efficiency (Figure 4c). This implies decreased combustion efficiency, accompanied by higher emissions, in the improved stoves (Table 2).

Combustion of dung cake, especially in the improved metal stove (typically with small combustion chamber volume), resulted in extremely high pollutant emissions. Compared to the traditional stove, improved stoves resulted in lower pollutant emission factors on a kW h^{-1} basis from wood combustion but in similar emission factors from briquette and dung cake showing enhanced emissions from these fuels even per useful heat input. Stoves should be designed with good emissions performance, for multifuel operation, as this is a user requirement.

Effect of Stove−Fuel Systems on Particle Size Distributions. Particle size distributions from all stove−fuel systems were unimodal with over 95% of the mass accounted in this mode (Figure 5a−c). The mass concentrations in each size range are given as Supporting Information (Table S1). All size distributions were unimodal with MMADs in the submicron range. For stoves S1, S3, and S4, these were 0.60−0.78 μm and showed similar mass size distributions of particle emissions from all fuels. However, in the case of stove S2 (improved single-pot stove), the MMADs from briquette and dung cake combustion were higher (0.77 and 0.74 μm) than that from wood (0.47 μm), showing larger average particle sizes from dung cake and briquette combustion.

No significant variation was seen between stoves S2 (improved one-pot) and S3 (traditional one-pot) in the PM emissions from dung cake and briquette combustion. However, for wood combustion, S2 resulted in both lower PM emissions and a lower MMAD or smaller average particle size. Both these point to more efficient combustion of the devolatilized organic compounds in S2. However, no statistically significant differences were found between S2 and S3, the traditional stove, for combustion temperature ($F = 0.01$, $p < 0.91$), burn rate ($F = 0.15$, $p < 0.70$), or power ($F = 0.60$, $p < 0.44$). A possible explanation for the more efficient

combustion of the volatilized organics is longer residence time or more complete mixing in the combustion zone in the improved stove S2, which had a larger fire-box volume and a grate providing primary air from the bottom of the fuel-bed. For stove design, this suggests the importance of providing sufficient residence time and turbulence in the fire-box for reducing PM emissions.

In these low-temperature biofuel combustion systems (800−1000 K), along with low updraft velocities, the ash in the fuels is not entrained and remains as residue on the grate. Particle formation during high-temperature coal combustion (*29*) has been seen to result in bimodal distributions of ash particles in a nucleation mode (0.01−0.1 μm diameter) and in a coalescence mode (2−10 μm diameter) at temperatures of 1500−2000 K. Soot particles (0.01−0.05 μm diameter) result from polymerization reactions of hydrocarbon free radicals during combustion of gaseous fuels or the volatilized components of liquid and solid fuels (*30*). We found unimodal size distributions of particles in emissions from biofuel combustion with MMADs of 0.5−0.8 μm, about a factor of 10 larger than those of typical soot particles from fossil fuel combustion (e.g., diesel) with potential implications for lung deposition and health risk. Examination of particle number concentration, morphology, and composition as a function of size is needed to investigate potential coagulation and condensation growth mechanisms.

Conclusions

Wood was the cleanest burning fuel, with higher emissions of CO from dung cake and PM from both dung cake and briquette fuels. Biofuel briquettes using cow dung as a binder resulted in fuel characteristics closer to dung cake than wood and consequently in higher emissions. The combustion characteristics of briquettes made with starch binder would be of interest. Combustion of dung cake, especially in the improved metal stove (typically with small combustion chamber volume), resulted in extremely high pollutant emissions. As a policy recommendation, it may be suggested that anaerobic digestion of dung to produce biogas be promoted as a substitute to low-temperature combustion of dung cake in stoves for cooking energy. Compared to the traditional stove, the improved stoves resulted in lower pollutant emission factors on a kW h^{-1} basis from wood combustion but in similar emissions from briquette and dung cake. Stoves must be designed for good emissions performance with multifuel capability, as this is a common user requirement. An improved one-pot stove, with a larger fire-box volume, gave lower PM emissions with smaller average particle sizes, suggesting the importance of providing residence-time and turbulence in the fire-box for reduced PM emissions. Unimodal size distributions of particles were measured in emissions from biofuel combustion with MMADs of 0.5−0.8 μm, about a factor of 10 larger than those of typical soot particles from fossil fuel combustion (e.g., diesel) with potential implications for lung deposition and health risk.

Acknowledgments

This work was supported by a research grant from the Centre for Indoor Air Research, MD, USA (Contract 97-12A). We thank M. Shekar Reddy and Ravindra Surve for help in establishing the Aerosol Research Laboratory. We appreciate the help of Gazala Parween and Tarun Gupta with experimental and data analysis work. We thank Appropriate Rural Technology Institute, Pune, India, for providing us the stove models. We deeply appreciate the insights and wisdom of several colleagues on aspects of the project over the past 3 yr. They include Dr. Veena Joshi (Swiss Development Cooperation, New Delhi), Dr. V. V. N. Kishore (Tata Energy Research Institute, New Delhi), Profs. Sangeeta Kohli and M. R. Ravi (Indian Institute of Technology, New Delhi), and Prof. Kirk R. Smith (University of California, Berkeley, CA).

Appendix

(a) Burn rate, F (kg h^{-1}):

$$F = \frac{1}{t}\left[\frac{(100W_{WD})}{(100+M)} + \frac{(W_K H_K)}{(H_W)} - \frac{(W_C H_C)}{(H_W)}\right]$$

(b) Thermal efficiency, η (%):

$$\eta = \frac{W_{wi}s(T_f - T_i) + (W_{wi} - W_{wf})L}{FtH_W}$$

(c) Power, P (kW):

$$P = \frac{FH_W}{3600}$$

Nomenclature

F = burn rate (kg h^{-1})
H_W = 15762 kJ kg^{-1}, heating values of wood
H_K = 43054 kJ kg^{-1}, heating values of kerosene
H_C = 28842 kJ kg^{-1}, heating values of charcoal
L = 2257.2 kJ kg^{-1}, latent heat of evaporation of water (at 298K)
M = moisture (%)
P = power (kW)
s = 4.18 kJ kg^{-1} K^{-1}, specific heat of water
T_i = initial temperature (K)
T_f = final temperature (K)
t = burn time (h)
W = wood
W_{WD} = weight of wood (kg)
W_K = weight of kerosene (kg)
W_C = weight of charcoal (kg)
W_{wi} = initial weight of water (kg)
W_{wf} = final weight of water (kg)
η = thermal efficiency (%)

Supporting Information Available

One table showing the aerosol mass concentration (mg m^{-3}) on each MOUDI stage for different stove−fuel systems. This material is available free of charge via the Internet at http://pubs.acs.org.

Literature Cited

(1) Ravindranath, N. H.; Hall, D. O. *Biomass, Energy, and Environment: A Developing Country Perspective from India*; Oxford University Press: Oxford, 1995.
(2) Sinha, C. S.; Sinha, S.; Joshi, V. *Biomass Bioenergy* **1998**, *14*, 489−503.
(3) Banerjee, R.; Inamdar, A. B.; Phulluke, S.; Pateriya, B. *Econ. Polit. Weekly* **1999**, 3545−3552.
(4) Kohli, S.; Ravi, M. R. *J. Solar Energy Soc. India* **1996**, *6*, 101−145.
(5) Davidson, C. I.; Lin, S.; Osborn, J. F.; Pandey, M. R.; Rasmussen, R. A.; Khalil, M. A. K. *Environ. Sci. Technol.* **1986**, *20*, 561−567.
(6) Smith, K. R. *Biofuels, Air Pollution, and Health−A Global Review*; Plenum Press: New York, 1987.
(7) Smith, K. R. *Annu. Rev. Energy Environ.* **1993**, *18*, 529−566.
(8) Saksena, S.; Prasad, R.; Pal, R. C.; Joshi, V. *Atmos. Environ.* **1992**, *26A*, 2125−2134.
(9) Zhang, J.; Smith, K. R.; Uma, R.; Ma, Y.; Kishore, V. V. N.; Lata, K.; Khalil, M. A. K.; Rasmussen, R. A.; Thorneloe, S. T. *Chemosphere* **1999**, 367−375.

(10) Ezzati, M.; Mbinda, B. M.; Kammen, D. M. *Environ. Sci. Technol.* **2000**, *34*, 578−583.
(11) Ahuja, D. R.; Joshi, V.; Smith, K. R.; Venkataraman, C. *Biomass* **1987**, *12*, 247−270.
(12) Gupta, S.; Saksena, S.; Shankar, V. R.; Joshi, V. *Biomass Bioenergy* **1998**, *14*, 547−559.
(13) Ballard-Tremeer, G.; Jawurek, H. H. *Biomass Bioenergy* **1996**, *11*, 419−430.
(14) Ballard-Tremeer, G.; Jawurek, H. H. *Biomass Bioenergy* **1999**, *17*, 481−494.
(15) Oanh, N. T. K.; Reutergardh, L. B.; Dung, N. T. *Environ. Sci. Technol.* **1999**, *33*, 2703−2709.
(16) Zhang, J.; Smith, K. R.; Uma, R.; Ma, Y.; Kishore, V. V. N.; Lata, K.; Khalil, M. A. K.; Rasmussen, R. A.; Thorneloe, S. T. *Chemosphere* **1999**, 353−366.
(17) VITA (Volunteers in Technical Assistance, Inc.). *Testing the Efficiency of Wood-Burning Cookstoves*; International Standards: Arlington, VA, 1985.
(18) U.S. EPA. Method 5 Sampling Train. *Code of Federal Regulations*, CFR 42, 1990.
(19) Hughes, T. W.; de Angelis, D. G. Emissions from Coal-fired Residential Combustion Equipment. In *Residential Solid Fuels: Environmental Impacts and Solutions*; Cooper, J. A., Malek, D., Eds.; Oregon Graduate Center: Beaverton, OR, 1982.
(20) Hildemann, L. M.; Cass, G. R.; Markowski, G. R. *Aerosol Sci. Technol.* **1989**, *10*, 193−204.
(21) Biswas, P. Measurement of High-Concentration and High-Temperature Aerosols. In *Aerosol Measurement: Principles, Techniques, and Applications*; Willeke, K., Baron, P. A., Eds.; Van Nostrand Reinhold: New York, 1993.
(22) Rao, G. U. M. Dilution Source Sampler for Measurement of Aerosol Size Distributions in Biofuel Stove Smoke. M. Tech. Thesis, Centre for Environmental Science and Technology, Indian Institute of Technology, Bombay, 1999.
(23) Sardar, S. B. Emission Factors of Respirable Aerosols and Particulate Polycyclic Aromatic Hydrocarbons from Biofuel Combustion. M. Tech. Thesis, Centre for Environmental Science and Engineering, Indian Institute of Technology, Bombay, 2000.
(24) Venkataraman, C.; Raman, P.; Kohli, S. *Energy Environ. Monit.* **1987**, *3* (2), 63−67.
(25) Joshi, V.; Venkataraman, C.; Ahuja, D. R. *Environ. Manage.* **1989**, *13*, 763−772.
(26) Joshi, V.; Venkataraman, C.; Ahuja, D. R. *Pac. Asia J. Energy* **1991**, *1*, 1−19.
(27) Prasad, K. K.; Sangen, E.; Visser, P. *Adv. Heat Transfer* **1985**, *17*, 159−317.
(28) Rohenow, W. M.; Hunsaker, J. P. *Trans. ASME* **1947**, *69*, 699−704.
(29) Flagan, R. C.; Friedlander, S. K. Particle Formation in Pulverised Coal Combustion: A Review. In *Recent Developments in Aerosol Science*; Shaw, D. T., Ed.; Wiley: New York, 1978.
(30) Flagan, R. C.; Seinfeld, J. H. *Fundamentals of Air Pollution Engineering*; Prentice Hall: Englewood Cliffs, NJ, 1988.
(31) Jenkins, B. M.; Jones, A. D.; Turn, S. C.; Williams, R. B. *Environ. Sci. Technol.* **1996**, *30*, 2462−2469.

Received for review August 18, 2000. Revised manuscript received February 20, 2001. Accepted February 26, 2001.

ES001603D